This is a repository copy of *Solid Biomass to Medium CV Gas Conversion With Rich Combustion*.

White Rose Research Online URL for this paper:
http://eprints.whiterose.ac.uk/160335/

Version: Accepted Version

GT2019-90196

SOLID BIOMASS TO MEDIUM CV GAS CONVERSION WITH RICH COMBUSTION

Gordon E. Andrews
School of Chemical and Process Engineering,
University of Leeds, Leeds, LS2 9JT, UK.

Aysha Irshad
University of Engineering & Technology,
Lahore, Pakistan.

Herodotos N. Phylaktou
School of Chemical and Process Engineering,
University of Leeds, Leeds, LS2 9JT, UK.

Bernard M. Gibbs
School of Chemical and Process Engineering
University of Leeds, Leeds, LS2 9JT, UK.

ABSTRACT

A modified cone calorimeter for controlled atmosphere combustion was used to investigate the gases released from fixed bed rich combustion of solid biomass. The cone calorimeter was used with 50 kW/m^2 of radiant heat that simulated a larger gasification system. The test specimen in the cone calorimeter is 100mm square and this sits on a load cell so that the mass burn rate can be determined. Pine wood was burned with fixed air ventilation that created rich combustion at 1.5-4 equivalence ratio, Ø. The raw exhaust gas was sampled using a multi-hole gas sample probe in a discharge chimney above the cone heater, connected via heated sample lines, filters and pumps to the heated Gasmet FTIR. The FTIR was calibrated for 60 species, including 40+ hydrocarbons. The hydrogen in the gas was computed from the measured CO concentration using the water-gas shift reaction. The exhaust gas temperature was also measured so that the sensible heat from the gasification zone was included in the energy balance. The GCV of the pine was 18.8 MJ/kg$_{pine}$ and at the optimum Ø the energy in the rich combustion zone gases was 14.5 MJ/kg$_{pine}$, which is a 77% energy conversion from solid biomass to a gaseous fuel feed for potential gas turbine applications. This conversion efficiency is comparable with the best conventional gasification of biomass and higher than most published conversion efficiencies for coal gasifiers. Of the energy in the gas from the rich combustion 35% was from the CO, 20% from hydrogen, 35% from hydrocarbons and 10% sensible heat. Ash remained in the rich burning gasification zone. As the biomass is a carbon neutral fuel there is no need to convert the gasified gases to hydrogen, with the associated energy losses.
.

INTRODUCTION

Solid fuels such as coal and biomass cannot burn directly in a gas turbine, they must first be gasified to syngas and the gas burnt in a combined cycle gas turbine, CCGT. The combined gasification and CCGT is referred to as integrated gasification combined cycle (IGCC). For clean coal the gasification gas can be converted to hydrogen using the water gas shift reactor and the residual CO_2 removed using carbon capture with solvent extraction. In principle the same can be carried out with biomass as the feedstock and then the plant has negative CO_2 emissions [1]. However, if biomass is the fuel then the carbon capture stage is not required as the fuel is deemed carbon neutral, provided sustainability criteria are met in the sourcing of the biomass. Thus, the electricity from biomass is renewable without the cost of carbon capture. To make CCS worth adding to a biomass IGCC plant would require legislation on carbon tax so that a financial benefit for negative CO_2 emissions plants can be achieved.

In most countries funding for renewable energy or zero carbon energy has not included carbon capture and storage, CCS, based clean energy. Introducing a carbon tax would be a way of promoting clean coal and negative carbon emissions would apply for biomass energy with CCS. The UK and the EU does not have a carbon tax as part of its carbon control strategy, which would apply to all uses of fossil fuels. In the UK there is a tax on coal for electricity generation, which has closed most coal fired power stations and all are due to be phased out by 2024. There is no carbon tax on natural gas use for electric power generation.

The EU and UK have chosen to reduce carbon emissions from electric power generation by mandating a specific proportion of electricity to be generated from renewable sources, irrespective of the cost. The additional cost of electricity generation from renewable sources is passed onto the

consumer in higher electricity prices. However, not all renewable sources are treated the same, as the UK Government decides which renewable technology is allowed to be used and allowed to charge higher prices to the Grid. For example offshore wind energy is supported and tidal power and solar (from March 2019) are not supported. Also nuclear electricity is treated as renewable, but fossil fuel with CCS is not. The subsidy for new Nuclear in the UK for Hinkley Point is over twice the current grid price for electricity, inflation adjusted. However, the policy has been successful as the current CO_2 emssions from the UK electricity grid are about $200 g_{CO2}/kWh_e$ compared with about 500 a decade ago. The cost to the consumer of this policy is about 20% extra electricity costs.

One of the approved renewable technologies for renewable electricity and heat in the UK and EU is biomass energy, provided strict biomass sustainability criteria are met in the biomass supply chain. In the UK in 2016 [2], pulverised biomass, used as a replacement fuel in previously coal fired powered generation plants, accounted for 7.35% of all electricity generated, which was up from 5.8% in 2014 [3]. Pulverised solid biomass was 30% of all renewable electricity generated in the UK in 2016 [2]. With the tax on coal plants are moving to 100% biomass and Drax power station, near Leeds in the UK, is the World's largest biomass power generator with 3GW of biomass based electricity. However, all of this biomass use is in steam cycle electricity plant converted from coal firing and none uses biomass IGCC, in spite of the higher thermal efficiency of the latter compared with 40+ year old coal fired steam plant. It would be preferable from a GHG reduction point of view if biomass was used in the most efficient power generation plant, which is modern combine cycle gas turbines.

The present work proposes smaller scale biomass gasification plant suitable for micro gas turbines. Applications would be in distributed electricity and in areas with no grid electricity such as rural areas in Pakistan and Nigeria. This research is directed at using a biomass combustion technology, known as gasification combustion or gasification boilers, that is widely used for heat production in Europe. This involves two stage rich/lean combustion of solid biomass and the present work proposes to direct the output from the rich gasification zone into a micro gas turbine for electricity production, rather than for heat production.

Biomass gasification on the small scale using micro-gas turbines for electricity generation is suitable for the local supply of distributed electricity. One area that needs this technology is countries such as Pakistan (4) where there is a poor distribution of electricity and no grid electricity in rural areas. Much of rural Africa also suffers from a lock of grid based electricity in rural areas. Rural areas have an abundance of agricultural waste material that could be used for electric power generation (4), but viable units would have to be on the scale of village needs and micro-gas turbines of <100kW$_e$ are feasible for this application. For individual large families a 10 kW$_e$ micro gas turbine would typically be required. The present rich burn gasification approach to converting biomass into a gaseous fuel could have applications in this area.

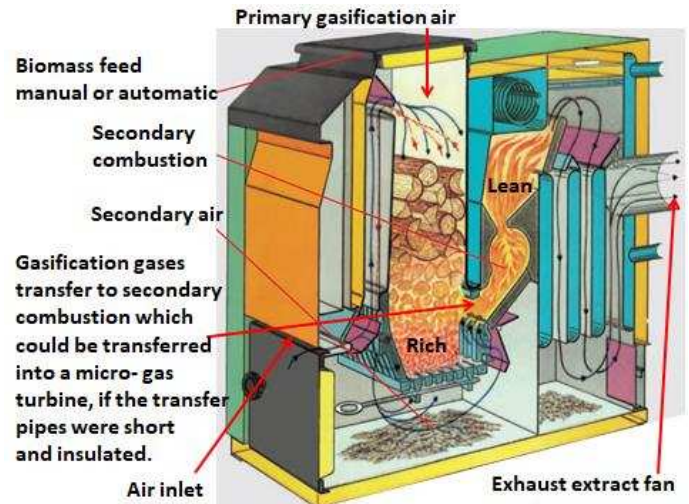Gasification boilers can burn raw unprocessed biomass, such as wood in log form. They can also be used with

Fig. 1 Typical log or gasification boiler for thermal power [5].

processed biomass such as pellets. The principle is two stage combustion with a rich burn first stage and then a transfer zone to a second stage combustion with air added to the efflux gases from the rich burn stage so that they then burn the gases in the secondary lean combustion zone. One example of this approach is shown in Fig.1. This shows a manual fixed split between the primary and secondary air. Some designs use a flap valve to enable the air split to be adjusted to improve performance for a particular biomass.

A problem with the simple thermal power application is that of the startup of the system which can be as simple as a manual fire start. The better systems have a gas burner start and dual gas/biomass operation offers benefits as the temperature of the gasification zone is easier to control. Where the zero carbon footprint is desired to be kept, a liquid biofuel burner could be used for startup or dual fueling. There is a large mass of solid biomass to heat before the desired evolution of gases occurs at a critical temperature, thus a separate burner to achieve this is desirable. In the present work this burner is replaced by an electrical radiant heater to raise the temperature of the biomass and control the air gasification zone temperature.

For gas turbine applications of this concept the rich burning gasifier would ideally be pressurized with compressor exit air. The high pressure gasified products, after particle filtration, would be fed hot as fuel to a low NOx gas turbine combustor. This would be designed with the required air splits for low calorific value (CV) gas that is generated in air blown rich burn gasifiers. It will be shown in this work that the highest energy conversion from biomass energy to evolved gas energy is critically dependent on the equivalence ratio, Ø, of the rich gasification zone. Biomass has a very wide ranging composition and each biomass has an optimum Ø$_{rich}$ that the air flow to the gasifier needs to be adjusted to achieve. Thus the air split between primary rich gasification combustion and secondary post air addition oxidation combustion is a variable that should depend on the biomass composition. Achieving this variable air split on a microgasturbine application is easier than on a boiler, such as that in Fig. 1, as a simple diverter valve can be used to control the air split from the compressor.

However, in practice virtually all biomass gasifiers use an atmospheric pressure air gasifier, as used in some coal IGCC plants such as at Duke Edwardsports [6]. The present test rig operated at atmospheric pressure and used air gasification. Annex 1 reviews some published work on biomass gasification and all are air based gasifiers and operate at atmospheric pressure. An atmospheric pressure gasifier for GT applications usually requires a compressor to compress the gasifier gas, ready to inject into the gas turbine combustor. In principle the gas could be injected into the air compressor and gas compression costs avoided. This has compressor fouling and particulate deposition issues, but could be viable in micro gas turbine where the risk would not be as great.

It is shown in this work, that uses lower gasification temperatures than more conventional biomass gasifiers, that a major proportion of the energy in the evolved gases are hydrocarbons. It will be shown that these are mainly ethylene, acetylene, benzene and toluene (there is no methane). Ethylene and acetylene are gaseous at ambient temperatures, but benzene and toluene could condense if the gasified gases are not kept at high temperature. Connecting hot gasified gases through insultated connecting pipework retains the sensible heat from the gasifier and this is important in the overall thermal efficiency. Losses of hydrocarbon by condensation (to produce tars) would deteriorate the overall efficiency of the gasifier and this has been a problem in some biomass and coal gasifiers. Annex 1 reviews some published data on biomass gasifiers and the present gasification technique with hot gas transfer from the gasification zone has one of the best gasifier thermal efficiencies in the literature as there are no losses of hydrocarbons.

The use of biomass for thermal power usually involves some form of two stage combustion, with the first gasification stage involving rich combustion to generate CO and H_2 and hydrocarbons, which are burnt in a second combustion stage by the injection of excess air at the second stage burner, as shown in Fig. 1. The equivalence ratio (Ø) of the primary rich burning stage, $Ø_{rich}$, required for the maximum gas conversion is usually not optimised. This research focuses on the optimization of the gas yield of the first stage of a two stage gasification system. The source of heat for the relatively small test samples is radiant heat and the work uses the cone calorimeter as modified by the authors [7]. This is the first time that the cone calorimeter has been used to characterize biomass gasification and combustion.

The Cone Calorimeter is shown in Figs. 2 and 3 and will be described in more detail later. Crucial in this work is its use with a controlled atmosphere around the heated specimen that enables different $Ø_{rich}$ to be achieved by varying the air flow. It is a common research method in Fire research, where it is used to characterise the ignition heat flux and the heat release rate of the tested materials, as well as to determine the toxic gas production [8, 9]. One of the most common fire materials is wood, as about 50% of all fires involve wood as the main fuel. The relevance to biomass combustion is then obvious. The cone calorimeter uses a conical electrical heater to heat the test specimen and is calibrated to be able to achieve 10 -70 kW/m^2 uniform heating of the test material. This radiant heat
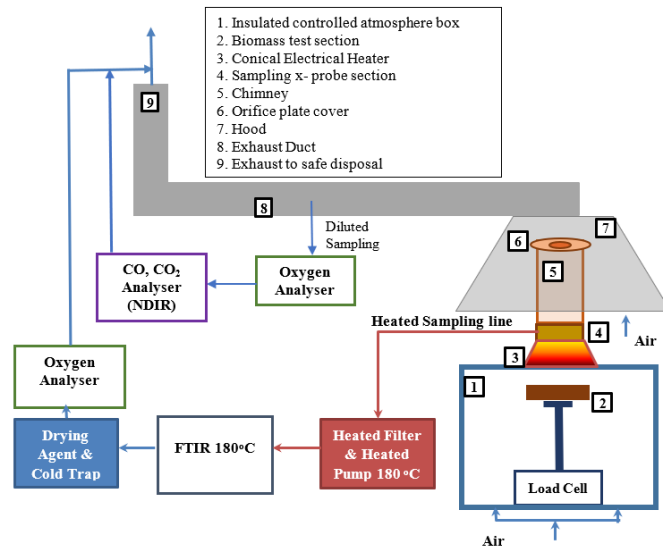

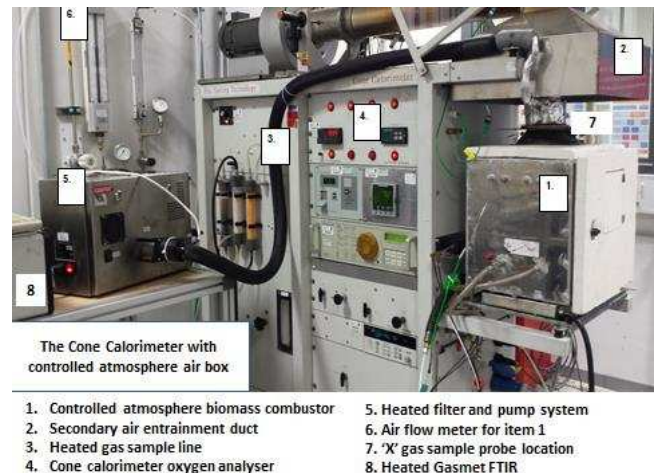Fig. 2 Cone calorimeter and flow sample system.

Fig. 3 Cone calorimeter and associated analytical equipment.

enables the biomass to be heated to ignition and also to control the temperature of the biomass combustion or gasification.

The radiant heat can be varied to determine the incident heat flux that will ignite materials and this is one of its applications to biomass combustion. The radiant heat represents the behaviour of the material in a fire surrounded by other flames that radiate to the specimen. It can thus be used with biomass using relatively small samples that are burning in the same way that they would in a much larger combustor biomass burning zone. A modification to the cone calorimeter enables a sealed box with a glass observation window to surround the test specimen. This enables the atmosphere around the test material to be controlled [10] and in this work was used with a controlled air supply to create rich burner gasification mixtures.

Some purpose built gasifiers, as shown in Annex 1, use pulverised biomass with stirred combustion zones, such as fluidised beds, to operate the gasification zone at a uniform temperature [6, 11], which is always a high temperature to ensure that all the biomass volatiles are released and it will be shown that this needs to be at least 800°C to release all the volatiles from pine wood. The present gasification method is

essentially a fixed bed gasifier with updraught air flow and a thermal profile in the solid wood is an essential part of the high effectiveness that is demonstrated in the results. A key difference from conventional gasifiers is that no steam is added, other than that in the logs as adsorbed water at the start of the gasification. There is always the raw original wood present, as more is added periodically, with a continuous release of volatiles into the rich burning zone. In the present work once the wood is ignited and burning downwards, the unburned wood below the burning surface is continuously releasing volatiles to pass through the char layer above. This process is also shown in Fig. 1, which is for a downward fixed bed gasifier.

BIOMASS COMPOSITION, VOLATILE RELEASE TEMPERATURE RANGE AND CHAR COMPOSITION

Pine wood was used as the biomass in the form of 20mm by 20mm square sections 100mm long with five of these placed side by side to make 100mm by 100mm test specimen. Some work on 40mm thick pine was also undertaken, mainly to show that 20mm thick test specimen was sufficient to produce a char layer with unburnt wood below that would release volatiles through the char. The water fraction, volatile fraction, fixed carbon and ash of the pine were determined using thermogravimetric analysis with nitrogen. A thermogravimetric analyser (TGA-50 Shimadzu with a TA60WS processor) was used. The procedures are explained by Saeed et al. [14].

The elemental analysis was carried out using a Thermo Flash EA 2000 oxygen combustion based elemental analyser which analysed for CO_2, H_2O, NO and SO_2 to determine the CHNS elemental composition and the missing mass was assumed to be oxygen. The instrument consists of a single reactor with temperature of 1800 ^{o}C for the detection of C, H, N and S. The oxygen content was calculated by subtraction of % CHNS and % moisture and ash (from the TGA) from 100. The elemental analysis is expressed on a dry ash free basis (daf). This is conventional solid fuel analysis and is also used for coal elemental analysis. The principle of assuming oxygen to be the missing mass has been applied for over 100 years in coal analysis and is the standard way of determining oxygen in biomass. A Parr 6200 oxygen bomb calorimeter was utilized for the determination of the gross calorific value of the pine.

The results for pine wood are shown in Tables 1 and 2. These show that for Pine there was 87% volatiles and Fig. 4 shows the volatile mass loss as a function of temperature for a range of biomass, which demonstrate that the pine used was typical of the range of biomass shown. 90% of the volatile mass loss in nitrogen occurs over the temperature range 250 – 500°C and it is these gases that are released and burnt with rich mixtures in the present work. At these temperatures there is no pyrolysis of the volatiles released from biomass and many biomass gasifiers use much higher temperatures with problems of pyrolysis of the gases to tars. If the volatile gases were burnt up to the 500°C pine temperature condition, then the mass of the biomass released as a gas would be 79% of the initial mass and this is what is burnt in the rich combustion zone. In the present work

Table 1 Elemental Analysis of Biomass (daf = dry ash free)

Biomass	Ultimate analysis, wt. %, daf					Stoich. A/F (g/g)	
	C	H	N	S	O	Actual	daf
Pine wood	48.4	6.1	0.2	0.0	45.4	5.3	5.7

Table 2 Proximate TGA Analysis of Biomass

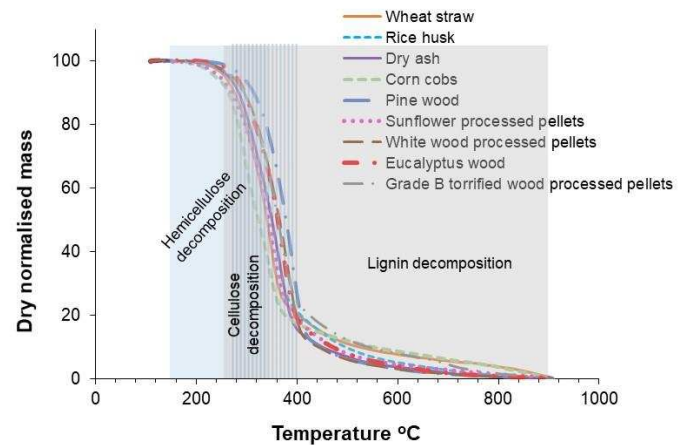| Biomass	Proximate analysis, wt. %				GCV MJ/kg	
	VM (daf)	FC (daf)	H_2O	Ash (ar)	Actual	daf
Pine wood	87.3	12.7	5.2	1.6	18.9	20.2

Fig. 4 Thermal gravimetric analysis of various biomass.

the composition of this gas and its energy content was determined by radiantly heating the sample in nitrogen and then burning it with rich mixtures to determine the products of rich combustion, which are the gases that would flow to the micro gas turbine.

The pine wood in the cone calorimeter was heated by radiation. A sample was tested with two thermocouples inserted at 3mm below the top surface and 3mm above the bottom surface. The measured temperatures as a function of time are
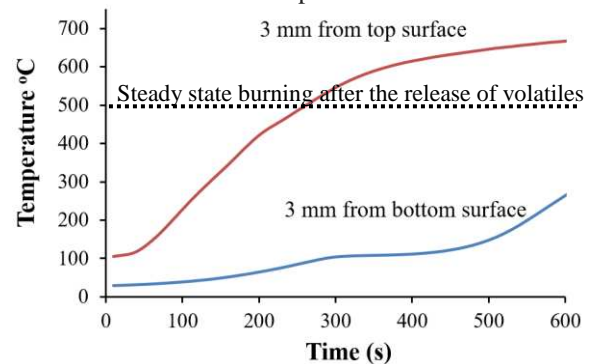

Fig. 5 Pine wood temperatures v. time for 70 kW/m^2 radiant heat and Ø$_m$ of 2.8 (air flow 19.2 kg/m^{2}s), for 20mm thick pinewood and 14mm separation between the top and bottom thermocouples.
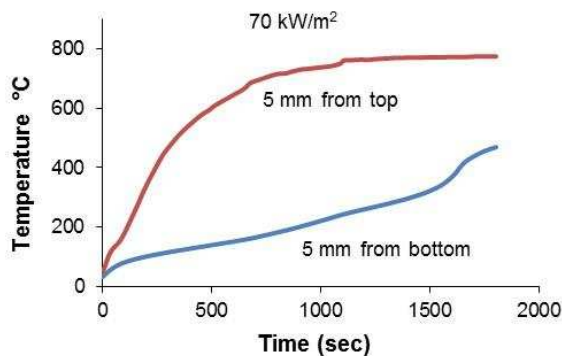
Fig. 6 Pine wood temperatures v. time for 70 kW/m² radiant heat and $\varnothing_m$ of 4.0 (air 12.8 kg/m²s), for 40mm thick pinewood and 30mm separation between the top and bottom thermocouples.

shown in Fig. 5 for 70 kW/m² radiant heating. These results and Fig. 4 show that the wood would release 90% of the volatiles over the time interval 100 – 300s, but would never reach pyrolysis temperatures of >800°C. 90% of the volatiles would be released once the pine temperature was above 500°C and the time to reach this is the light up phase of the reaction. In this work, results are reported for steady state burning which occurs once the pine is at 500°C or above and 90% of the volatiles have been released. The equivalence ratio $\varnothing_m$ under the steady state burning conditions after 500°C has been achieved is used to correlate the composition of the product gases which would flow as fuel to the micro gas turbine combustor.

Fig. 5 also shows that the conduction of heat through the wood was a relatively slow process and volatiles would continue to be released from the bottom of the wood well after the top surface was at 600°C. This is a key feature of log gasification boilers: the logs continue to release volatiles for hours, in the presence of an outer char layer.

For longer heating periods Fig. 6 shows for 40mm thick pine wood that the top surface temperature increased to 750°C which was a stable final temperature in the test after 1200s. Fig. 4 shows that at 750°C 100% of the pine volatiles had been released, so that from Table 2 there would have been 87% of the initial biomass mass released as volatiles. This test was a lower air flow rate of 12.8 kg/m²s which will be shown later to create richer combustion with a similar flame temperature to that at $\varnothing_m$ in Fig. 5. This explains why the two surface temperatures were similar for different $\varnothing_m$.

The temperature 30mm below the upper temperature for the same time was similar to that in Fig. 5, but increased to 500°C after 1750s. For all of this period the lower cooler wood had been releasing volatiles that passed through the upper layer char and this is why the gas conversion, as shown later, is so high for this type of rich burn solid biomass gasification.

The lower temperature of the pine wood is influenced by downward heat losses to the metal support rod and then to the water cooled load cell enclosure. The impact of this on the top reaction zone temperature is shown in Fig. 7, which shows a gain of about 50°C when a 20mm thick insulation board was placed below the 20mm thick pine, compared with 40mm uninsulated pine wood. This was preferable to using 40mm
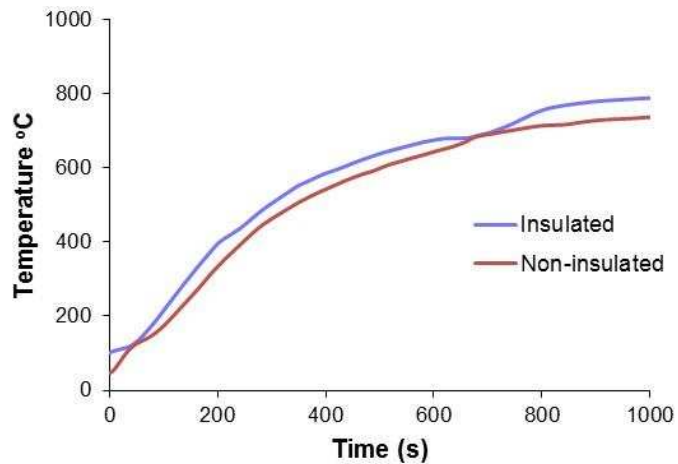

Fig. 7 Pine wood temperatures v. time for 70 kW/m² radiant heat and $\varnothing_m$ of 4.0 (air 12.8 kg/m²s), for 40mm thick pinewood with the top thermocouples 5mm below the surface. The insulated results are for 20mm thick pine and 20mm insulation underneath.
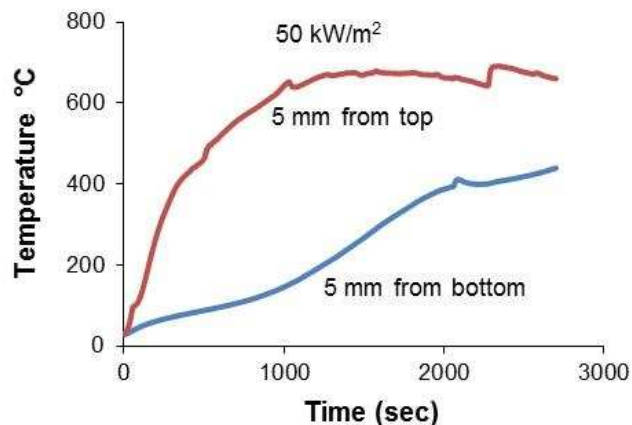

Fig. 8 Pine wood temperatures v. time for 50 kW/m² radiant heat and $\varnothing_m$ of 2.8, for 40mm thick pinewood and 30mm separation between the top and bottom thermocouples at $\varnothing_m$ = 4.0 (air 12.8 kg/m²s).

thick wood sample and also reduced the test time as there was only 20mm thickness of pine to burn. In all the results in the present work the 20mm thick insulation was in place below the test material. Effectively this made the 20mm thick test specimen behave as an infinitely thick specimen in the initial burning phase.

Fig. 8 shows the upper and lower temperatures in 40mm thick pine for a lower radiant heating of 50 kW/m². The results are similar to those in Fig. 6 with an equilibrium upper temperature of 670°C after 1200s. This is lower than the 750°C after 1200s in Fig. 4, indicating, as expected, that a higher radiant flux will produce higher surface temperatures. However, Fig. 4 shows that at 670°C 95% of the volatiles will be released, which is close to that of 100% at the 70 kW/m² radiant flux. Fig. 8 also shows that the bottom temperature does not start to rise above 250°C for the onset of volatile release until after 1500s, compared with 1200s in Fig. 6 and 600s in Fig. 5. It is clear that the thicker the wood the longer will the top char layer

be exposed to a flow of volatiles from the raw wood beneath the char. As the physics of volatile release and char formation were already present in the 20mm thick pine wood, this was the thickness that was used in most of the present work

Figs. 5, 6 and 7 show that gases are evolved from the base of the wood and have to pass through the upper char layer where they are heated. The CO and H_2O released from the cooler wood passes through the char layer at the top and this can promote char reactions with H_2O to produce more CO and hydrogen. Table 3 shows the elemental and TGA analysis of the char that remained at the end of the test in Fig. 5. The fixed carbon is 88% but there is still a significant volatile fraction which will be located in the base of the char as this will have been at high temperature for a shorter time. Fig. 4 shows that the residual volatiles will be lignins that require temperatures of 800°C to remove completely. Table 3 also shows that the char has a higher energy content than the original biomass and has a much higher stoichiometric A/F.

Table 3 Elemental and TGA Analysis of the top char

Parameter	Pine char (top layer)
Carbon	97.1
Hydrogen	2.5
Nitrogen	0.10
Sulfur	0.00
Oxygen	0.35
Volatile matter	12.3
Fixed carbon	87.7
Moisture (% ar)	4.1
Ash (%ar)	6.9
Stoichiometric (A/F) dry basis	12.0
Stoichiometric (A/F) wet basis	10.7
GCV (MJ/kg)	34.0

Table 4 Reactions that can occur between the volatile rich combustion gases and char.

Reaction	Energy (+ is endothermic)	Reaction name
$C + CO_2 \leftrightarrow 2CO$	$\Delta H_r = +172 \frac{kJ}{mol}$	Boudouard Reaction
$C + H_2O \leftrightarrow H_2 + CO$	$\Delta H_r = +131 \frac{kJ}{mol}$	Steam gasification of carbon
$C + 2H_2 \leftrightarrow CH_4$	$\Delta H_r = -75 \frac{kJ}{mol}$	Carbon Hydrogenation / Methanation/ Hydrogasification

The gases from below the char from the rich combustion flow through the char layer at the top and can undergo reactions with char that are summarized in Table 4. The main products of rich combustion, CO_2, H_2O and H_2 can all react with char to form increased CO and hydrogen. In large uniform temperature gasifiers the biomass are injected as fine particles and there are no thermal gradients in the particles and they all have to be hot enough to drive off all the volatiles. In this case steam is injected to promote the steam gasification reaction in Table 4 and produce increased hydrogen. In the present solid biomass rich burn gasification, the water in the biomass can undergo the same reactions as it passes through the char layer. This is one of the reasons that the high performance shown in the present results, without steam injection, show the effectiveness of the interaction of the volatile release with the char.

CONE CALORIMETER

For the present work, a modified controlled atmosphere cone calorimeter was used, with a sealed air box around the burning biomass and the air supply controlled so that $\emptyset_m$ could be varied by varying the air flow. The original version of this cone calorimeter equipment had considerable development before it was used in the present work [7]. The development centered on two aspects: firstly, heat losses to the metal box and load cell metal support were excessive and lowered the reaction zone temperature; secondly, the measurement of the mean composition of the outlet gases from the cone chimney was a problem due to the non-uniform flame and to oxygen backflow into the discharge pipe, caused partially by the extract flow of the FTIR sample (4 lpm) [7].

In order to avoid heat losses to the enclosure box, 25 mm thick insulation board was used to insulate the walls. The top surface and the door were insulated from outside, while the rest of the box was insulated from the inside. After insulation, the internal dimensions of the box were 33 cm long, 27.5 cm wide and 30.5 cm high. A metered flow of air was supplied to the sealed box from two openings in the bottom. A calibrated variable area flow meter was used to determine the flow rate of air so that the metered equivalence ratio, $\emptyset_m$, of the combustion could be controlled. The mode of gasification is usually referred to as fixed bed updraught gasification. This is because the biomass to be gasified is solid in its raw form and has a fixed location and is not agitated as in some gasifiers such as fluidized bed gasifiers which operate at a constant temperatures throughout the bed. The air flow goes upward from the bottom of the test chamber over the test section and up the chimney, so it is an updraught gasifier. Commercial gasification or log boilers are all fixed bed gasifiers in the primary stage but can be either downdraught, as in Fig. 1, or updraught as in the present experiments and several commercial log boilers [5].

The biomass used in the present work was 5 sticks of pine of square dimension 20mm and 100 mm long and placed in the 100 mm square test section of the cone calorimeter, as shown in

Fig. 8 The 5 20mm square pine wood test material.

Fig. 9 View of a typical biomass flame through the chamber observation window

Fig. 10 The 20 holes mean gas sampler

Fig. 8. For other biomass the wood could be round with bark attached or in pellet format. The conical electrical heater was a 65mm long, truncated cone with 80 & 177 mm diameter top and bottom openings and was attached to the top of sealed box. An 80mm diameter exit pipe or chimney was attached to the exit plane of the cone and this was the gas sample location for all the gasification product analysis in the present work.

The problem of achieving a mean gas sample with no oxygen dilution from entrained air from the chimney exit was difficult to solve and the solution may still not be adequate [13]. The problem can be seen in the biomass flame photograph in Fig. 9, which shows the flame is located in the centre of the outlet surrounded by cooler gases and is clearly not mixed. This photograph was taken through an observation window mounted in the door of the chamber. This has an insulation block placed over it when the flame was not being observed.

The best solution to the mean gas sample problem was to use an 'X' probe with 20 gas sample holes on centres of equal area as shown in Fig. 10. This was mounted in a 40mm long 76mm diameter duct that was placed at the cone heater outlet. An insulated metal chimney 210 mm high and 80 mm inside diameter was placed on the top of the 'X' probe sampling section. The chimney exit was covered with a perforated plate with a 90% blockage of the exit to prevent the back flow of

external air inside the chimney. The problem of air backflow was shown by the presence of significant oxygen levels in the mean gas composition when the combustion zone was supposed to be operating very rich. For rich combustion zero oxygen was achieved with the mean gas sample, demonstrating that no external air had been entrained into the sample flow.

In spite of the use of a 20 hole mean gas sample probe, it is possible that this did not achieve an accurate mean sample. The difference between the carbon balance $\emptyset_e$ and the metered $\emptyset_m$ was significant and $\emptyset_m$ was always richer than $\emptyset_e$ apart from at the highest air flow rates and lowest $\emptyset_m$ as shown in Fig. 11. This indicated that the mean gas sample was oversampling the air surrounding the flame in Fig. 9. In all of the results in this paper the metered equivalence ratio, $\emptyset_m$, is used.

This rich primary zone combustion had a heat release determined by oxygen mass consumption using the metered air flow rate and its oxygen content to determine the oxygen mass flow consumed in the rich combustion reactions. The paramagnetic oxygen analyser was located in the sample flow after the FTIR and the water in the hot sample was first condensed so as to measure the oxygen on a dry basis. The oxygen consumption calorimetry needs the oxygen mass flow and a wet based oxygen measurement is required. This was determined using the water vapour measurement of the FTIR on the hot gas sample to convert the dry gas oxygen measurement to a wet gas concentration.

The rich gasification gases from the chimney flowed to the exhaust duct of the cone calorimeter, where air was entrained and secondary combustion occurred. The global heat release rate, HRR, was determined by oxygen consumption in the cone calorimeter exhaust duct. The difference in the overall and primary HRR gave the HRR for secondary combustion. However, the focus of the present work was on the primary rich gasification combustion.

To record the sample temperature of the wood two 1.5mm thick type K thermocouples were inserted from the side wall of the enclosure box with the tip on the centreline of the central wood stick at 3mm from the top and 3 mm from bottom surface of the pine stick. The insertion of thermocouples lifted wood and gave a false weight and these tests were carried out separately from the mass loss measurements. Typical wood temperature records are shown in Figs. 4-7.
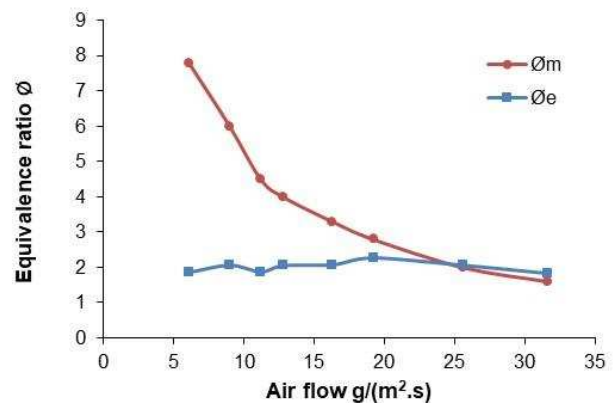

Fig. 11 Comparison of metered equivalence ratio $\emptyset_m$ with emission based equivalence ratio $\emptyset_e$ for pine wood tests
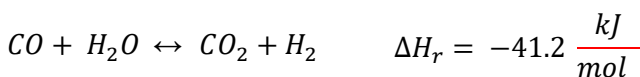
HEATED FTIR GAS COMPOSITION ANALYSIS

The gas sample from the 'X' mean gas sample probe was pumped via a heated PTFE tube to a heated filter and pump system and then via a further heated line to a heated Gasmet CR-series FTIR spectrometer. The temperature of the heated filter, pump, and heated line to and from the pump was maintained at $180^{\circ}C$ to keep the hydrocarbon volatiles in the gas phase so that there were no compound losses in the analytical system.

This Gasmet FTIR is a purpose-built portable unit that has UK Environmental Agency MCERT approval for legislated flue gas composition measurements. It has been available for over 20 years and other manufacturers have similar instruments. This is today a routine instrument for complex gas composition measurements. It was calibrated by the manufacturer for 60 gaseous species and does not need further calibration. Calibration was checked for some gases, CO_2, CO, benzene, methane, propane, hexane using certified bottles and the agreement was satisfactory [14-15]. The only thing needed prior to the test was to zero the instrument on nitrogen. This FTIR has been used for in vehicle real world exhaust gas measurement as well as in large scale compartment fires [16, 17].

The Gasmet FTIR analyzer has a liquid nitrogen cooled MCT (mercury-cadmium telluride) spectrometer detector, which enables the resolution of 8 or 4 cm^{-1}, with a minimum scan frequency of 10 Hz. It covers the wave number range from 600 to 4200 cm^{-1} and gives $0.3 – 2$ ppm minimum detection limits, depending on the gas. As it is fully heated it measures the total water vapour present in the sample. The recorded FTIR sample spectra were analysed using Calcmet software. Calcmet can analyse the sample for more than 50 components. However, it is not recommended to analyse more than 50 components at one time for the best accuracy of analysis [18]. There is no requirement to examine individual gas absorption spectra in the quantitative use of this analyser, although full spectra are recorded. The gas sampling, calibration and species quantitation complied with the ISO standard [19] that applies for the use of FTIRs for toxic gas analysis in fires.

H_2 does not absorbed infrared radiation and cannot be detected by FTIR. It was calculated from the water gas shift reaction, as in equilibrium with the CO measurements.

$$CO + H_2O \leftrightarrow CO_2 + H_2 \qquad \Delta H_r = -41.2 \, \frac{kJ}{mol}$$

The equilibrium constant for this reaction is:

$$K = \frac{[CO][H_2O]}{[CO_2][H_2]}$$

A K value of 3.5 was used, which corresponds to T_{eq} 1738 K [20, 21]. This procedure to determine the hydrogen content in rich combustion from the CO measurements has been in use in the automotive industry for over 50 years [20], as rich combustion occurs in SI engines. It is recognized in SAE (H-2400) and ISO (ISO 8178-1) standards for gas analysis processing. Thus this method for the calculation of hydrogen

from CO in rich mixture is reliable and has been in use in gas analysis processing for many years. Hydrogen is a difficult gas to measure on-line and so in gas analysis for rich mixtures hydrogen is always calculated in this way.

Downstream of the FTIR gas outlet was a water cooler and silica gel column to remove any condensates and water vapour present in the sample. This dry gas sample was then fed to a paramagnetic oxygen analyzer for the measurement of oxygen in the gas sample from the raw gas sample chimney 'X' probe and for the determination of the heat release rate (HRR) of the gasification zone by oxygen consumption calorimetry. A complete schematic of the cone calorimeter and gas analysis sampling system is shown in Fig. 2 and the complete system is shown in Fig. 3. The water vapour measured by the FTIR was also used to correct the oxygen reading from a dry to a wet gas basis prior to the oxygen consumption calorimetry calculations.

VOLATILE GAS COMPOSITION FROM HEATED BIOMASS IN NITROGEN

The TGA analyser that produced the results in Fig. 4 cannot be used with the present FTIR as the required sample flow rates are greater than those used in the TGA analyser. An alternative method, that is equivalent, is to operate the cone calorimeter with a controlled atmosphere of nitrogen. The radiant heater will heat the biomass and release volatiles that now do not react as there is no oxygen in the gas. The nitrogen flow rate was set at the same flow as the air flow with gasification reactions, so that the convective removal of the gases from the biomass surface was the same as with air flow. Thermocouples 5mm below the top surface and 5mm above the bottom surface of the pine were used to determine the biomass temperature and thermal gradients. The mass loss of the pine due to the evolution of volatiles is shown in Fig. 12 for radiant heating from $10 – 25$ kW/m^2. This show that at 25 kW/m^2 there was 72% of the mass evolved as volatiles. This compares with 87% in Table 2 on a daf basis which converts to 81% on an actual basis, which is only 4% different from that in Fig. 12, but it is possible that a higher radiant heat flux is required to fully devolatilize the pine.

Figs. 13 and 14 show the top and bottom thermocouple temperatures for pine for a range of radiant heating from $10 – 25$ kW/m^2. This shows as expected that the equilibrium surface temperature is a function of the radiant heating and at 25 kW/m^2 $480^{\circ}C$ was achieved and slightly below this at 20 kW/m^2. At 25 kW/m^2 the time to heat the 20mm thick pine wood is 1700s to steady state, but the loss of volatiles starts at $250^{\circ}C$, as shown in Fig. 4. Fig. 14 shows the bottom temperature reaches $470^{\circ}C$ after 1700s and then increases much more slowly. At earlier times comparison of Figs.13 and 14 shows that the bottom temperature lags the top temperature, as shown in Figs. 5, 6 and 7 for the combustion case. Fig. 15 compares the mass loss rate on the cone calorimeter in nitrogen with that derived from Fig. 4 using the TGA in nitrogen.

The TGA used small samples of powdered pine and could be assumed to be at a uniform temperature at each time interval. In contrast Figs 13 and 14 for the cone calorimeter tests show a difference in the top and bottom pine stick
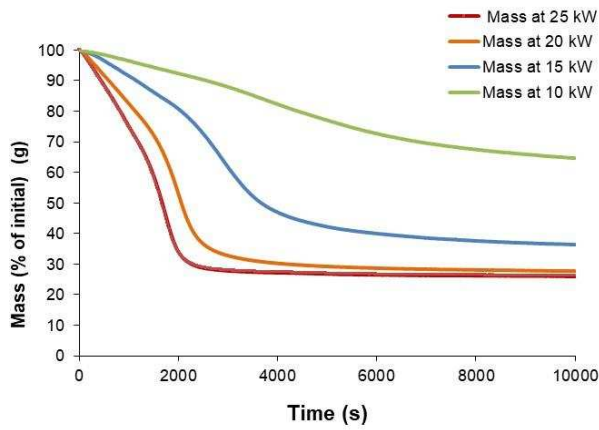
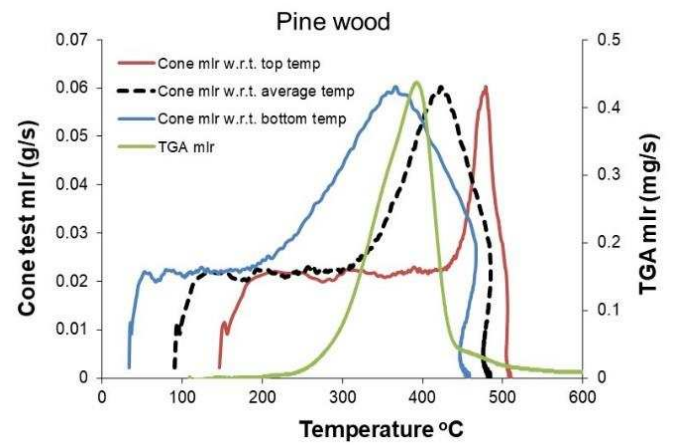Fig. 12 Mass loss v. time for 10 – 25 kW/m^2 radiant heating in nitrogen.

Fig. 13 Temperature 5mm from the top pine surface, for radiant heating from 10 – 25 kW/m^2.

Fig. 14 Temperature 5mm from the bottom pine surface for various biomass including pine wood, for 10 – 25 kW/m^2 radiant heating.

temperature during the heating period. After 2000s at steady state for 25 kW/m^2 heating the top temperature was 530°C and the bottom was 450°C. Fig. 4 shows that 95% volatiles should have been released from the top surface at this time and 85% from the bottom surface.

Fig. 15 shows the rate of mass loss as a function of the top and bottom temperature and of their mean. The cone

Fig. 15 Comparison of the mass loss rate for a cone test with that of the TGA mass loss rate vs time for pine wood.
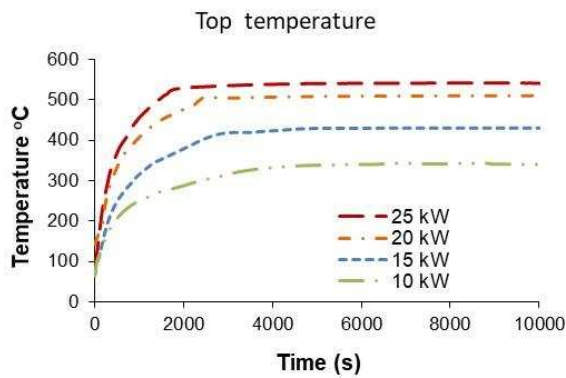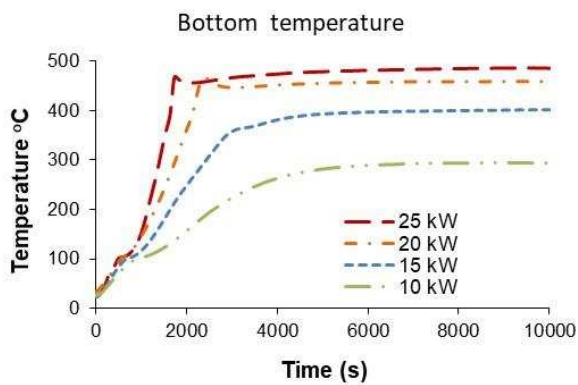

Fig. 16 Cumulative volatile gas yields from FTIR analysis at 25 kw/m^2 radiant heating in nitrogen.

Fig. 17 Cumulative total mass loss: comparisons of the load cell measured mass loss with the mass of the evolved gases from the FTIR analysis.

calorimeter results in nitrogen show a poor agreement with the TGA results, but the best agreement is with the mean wood temperature. The biggest difference is the mass loss at lower temperatures and part of this difference is that Fig. 4 excludes water vapour removal, whereas for the cone calorimeter the

Copyright © 20xx by ASME

weight loss includes water. However, in the region above 150°C, where the water has been evaporated throughout the thickness of the wood, there are still differences with the TGA. This shows that the heating of thick wood in log gasifiers is different from the uniform temperature on the TGA and in fluidized bed gasification.

Fig. 16 shows the accumulative mass from the FTIR with a breakdown of the gases that contribute to this mass. Fig. 17 shows good agreement between the mass loss on the load cell and that calculated from the FTIR measured concentrations converted to mass yields. This indicates that the FTIR calibration is good and includes all the significant species in the volatile gases from heating the pine wood. In Fig 16 the 'others', which are 15% of the yield, are all hydrocarbons with a similar GCV. The presence of H_2O and CO_2 at 37% of the mass lowers the calorific value of the gas. The other main volatile gases were xylene (4%) trimethyl-benzene (5%), formaldehyde (2%), acetic acid (2%), acrolein (1%) and furfural (1%).

Fig. 18 shows the energy content of the evolved gases as a function of time for 25 kW/m^2 radiant heat. Initially the HHV was low, due to the absorption of biomass heat release in the vaporization of water in the pine over the first 2000s. After 2000s the HHV increased and an average value of HHV from 2000 to 10000 s for tests at 10, 15, 20 and 25 kW/m^2 was 14.3, 13.9, 15.5 and 14.4 MJ/kg respectively.
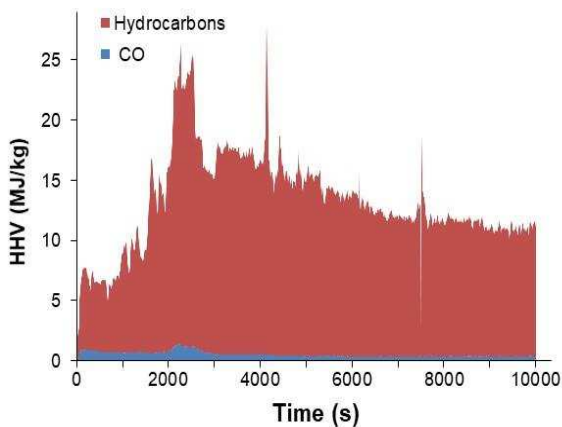

Fig. 18 Calorific value (HHV – MJ/kg$_{gas}$) of the evolved gases as a function of time for 25 kW/m^2 radiant heat.

Table 5 compares the elemental composition of the initial biomass and the final char over the 10 -25 kw/m² radiant heating range. The difference in the elemental composition is shown and compared with the total volatile mass released from the FTIR analysis. The difference is the mean elemental composition of the gases that were evolved. Comparison with the same mean composition from the FTIR shows good agreement for 20 and 25 kW/m^2, but there were larger differences at lower radiant flux. These results show that the FTIR gas composition analysis is reliable.

Table 6 shows the mean HHV of the gases evolved and the char, together with the proportion by mass of gas and char. The HHV of the two components are used to determine the energy split between the gases and the char. The proportion of the

Table 5 Comparison of the initial biomass and final char elemental composition with that deduced from the FTIR analysis, on an as received basis (ar).

25 kW/m² 114.49 g	Wood 114.49 g	Char 29.84 g 26.1%	Difference (g)	Elements from FTIR (g)
C	51.61	23.37	28.25	31.98
O	48.40	1.38	47.02	50.90
H	6.50	0.97	5.53	6.85
N	0.23	0.03	0.20	0.23
20 kW/m²	Wood 117.94 g	Char 32.62 g 27.7%		
C	53.17	24.96	28.21	32.76
O	49.87	4.73	45.14	49.59
H	6.70	1.24	5.46	6.70
N	0.24	0.04	0.20	0.19
15 kW/m²	Wood 118.3 g	Char 43.0 g 36.3%		
C	53.33	24.32	29.01	25.84
O	50.01	14.66	35.35	44.81
H	6.72	2.30	4.42	6.11
N	0.24	0.02	0.22	0.20
10 kW/m²	Wood 116 g	Char 74.9 g 64.6%		
C	52.29	42.37	9.93	14.88
O	49.04	23.05	25.99	23.60
H	6.59	4.00	2.59	3.11
N	0.23	0.03	0.20	0.13

original biomass energy that is in the gas is quite low, but similar for 20 and 25 kW/m^2. If a gasifier only produced this proportion of gas and then burnt it, the overall thermal efficiency would be poor. It will be shown that with rich combustion a higher proportion of the biomass energy was transferred into the gas and the implications is that the reactions in Table 4 take place and convert more of the char into gas. It will be shown that there was little methane produced and so the third reaction in Table 4 must be negligible.

EQUILIBRIUM RICH COMBUSTION CALCULATIONS

The CEA (Chemical Equilibrium and Applications) software by NASA was used to perform the thermodynamic equilibrium calculations of the gasification of biomass to predict the composition of gases and the adiabatic flame temperature as a function of equivalence ratio Ø [22]. The programme calculates equilibrium compositions using a Gibbs Free Energy minimization method. The software uses input information: temperature, pressure, enthalpy, entropy, internal energy, specific heat capacity and mole fractions of the reactants for calculation of the output data at equilibrium for every mole of mixture. The elemental composition of the components C, H, N and O in the biomass and the GCV, as shown in Table 1, were the input to the calculations.

Table 6 Comparison of energy content of the evolved gases and the residual char expressed as MJ/kg of original biomass.

25 kW/m²	HHV MJ/kg	% Yields ratio	Energy MJ/kg biomass	Energy in gas as % of energy in biomass
Gases	13.9	72.5	10.1	53.5%
Char	31.1	27.5	8.6	45.5%
Total			18.6	
20 kW/m²				
Gases	14.5	71	10.3	54.5%
Char	30.6	29	8.9	45.5%
Total			19.2	
15 kW/m²				
Gases	13.1	62	8.0	42.3%
Char	27.0	38	10.4	57.7%
Total			18.4	
10 kW/m²				
Gases	13.5	32	4.3	22.8%
Char	21.4	68	14.6	77.2%
Total			18.9	
GCV of Pine wood 18.9 MJ/kg				

The equilibrium compositions as a function of Ø for pine wood using CEA software are shown in Fig. 19. The maximum concentration of CO (about 25%) and CO plus hydrogen (about 47%) was achieved between 3 and 3.5Ø. Fig. 19 also shows that no significant hydrocarbons were predicted at equilibrium until Ø > 3.5. Thus, the presence of hydrocarbons in experimental rich combustion of biomass is an indication that the gasifier is not operating adiabatically. This was why in the present work insulation of the gasification zone to minimize heat losses was important. This equilibrium composition illustrates that for gasification the optimum operating conditions for the maximum flammable gas composition will vary with the biomass composition, due to variation in the CHONS elemental composition. This means that the primary air flow will need to be adjusted for each biomass to hold the gasifier at optimum $Ø_{rich}$. In this work this optimum was found for pine wood.

Fig. 19 shows that at the point of maximum yield of CO and hydrogen the adiabatic temperature is ~800°C for pine wood. This gives a possible control option for the primary zone air flow. The primary air flow could be reduced until the exit temperature stopped declining and adopted a near constant temperature, as shown in Fig. 19, with a very slow reduction in temperature as the mixture becomes richer.

Figs. 5-8 show that towards the end of the recorded period the temperature close to the top of the pine wood was 670°C at $Ø_m$ = 2.8, which is close to the optimum for maximum energy in the evolved gases, as will be shown later. This is below the adiabatic temperature of 800°C, shown in Fig. 19, due to combustion inefficiency and heat losses.
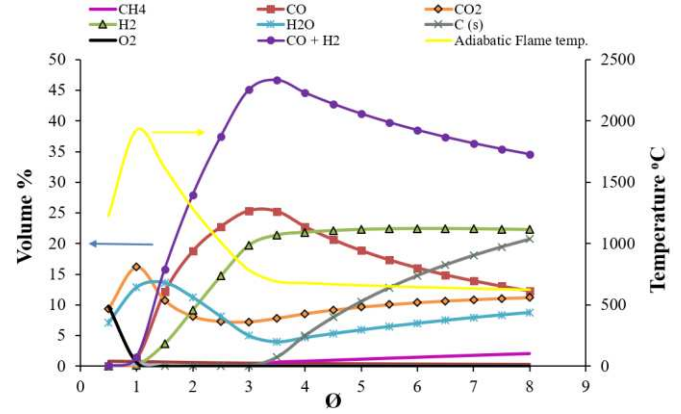

Fig. 19. CEA predictions of equilibrium conditions as a function of Ø for pine wood.

MASS CONVERSION TO GAS, PRIMARY HRR AND GASIFICATION ZONE $Ø_m$

Tests were performed with air flowing into the controlled atmosphere box around the test material, at a radiant heat flux on the cone calorimeter of 70 kW/m², for different air flow rates with pine wood. The measured air flow rate in lpm was converted into g/m²s to make it possible to scale up the results to practical equipment size. The air mass flow rate per surface area, g/m²s, is based on the test specimen flat surface area of 0.1m x 0.1m. This can be converted to kW/m² by multiplying g/m²s by 3.05 kJ/g_{air}. This uses the concept of the heat release per kg of air being constant for any fuel that is burnt. The constant normally used is 3.05 MJ/kg_{air} which converts to 13.1 MJ/kg_{oxygen} and assumes complete combustion. 13.1 MJ/kg_{oxygen} is the constant used in oxygen consumption calorimetry [23]. Oxygen consumption calorimetry is used in the present work to determine the HRR in the primary and secondary combustion zones on the cone calorimeter.

The metered fire equivalence ratio, $Ø_m$, was determined from the rate of pine wood mass consumption from the load cell and the metered air flow, which gave a measured A/F by mass. The stoichiometric A/F was determined from the elemental analysis and given in Table 1. The equivalence ratio $Ø_m$ is the ratio of the stoichiometric A/F to the metered A/F.

There was an ignition delay of 97s between the start of radiant heating and the ignition of the pine wood at the 19.2 kW/m²s air flow rate. All the graphs with a time scale refer to the time from pine wood ignition.

Fig. 20 shows the primary and secondary HRR as a % of the total HRR for the first 600s of the rich burn biomass combustion. Combustion in the primary rich burn gasification stage was at steady state after 300s and other emissions measurements were also constant after 300s. This is the same time as to reach 500°C in Figs.5-7. After 600s with 20mm thick pine, char combustion started to be important. It was desired in this work only to investigate the rich burn combustion of the volatile gases, as in a practical combustor fuel would be added periodically to keep the production of volatile gases as a continuous stream. Also for longer test periods the load cell started to overheat.
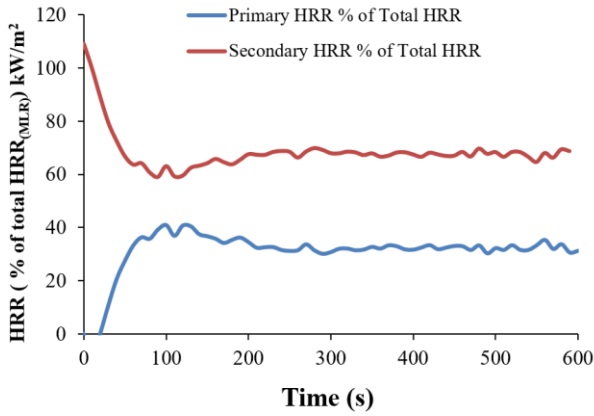
11   Copyright © 20xx by ASME

Fig. 20 Primary and secondary HRR as a % of the total HRR for pine wood at 70 kW/m^2.

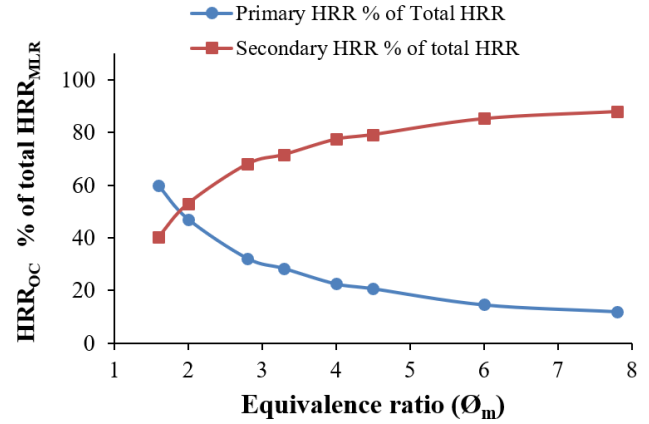Fig. 21 Equivalence ratio as a function of primary air flow

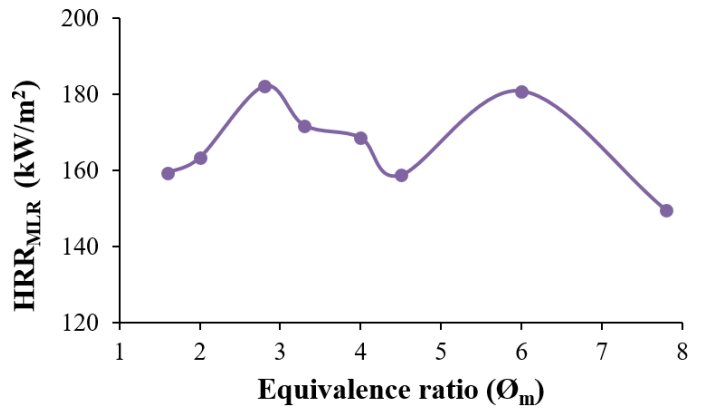Fig. 22 Primary and secondary HRR as % of total HRR $_{(MLR)}$ (kW/m^2) for tests with different airflow rates

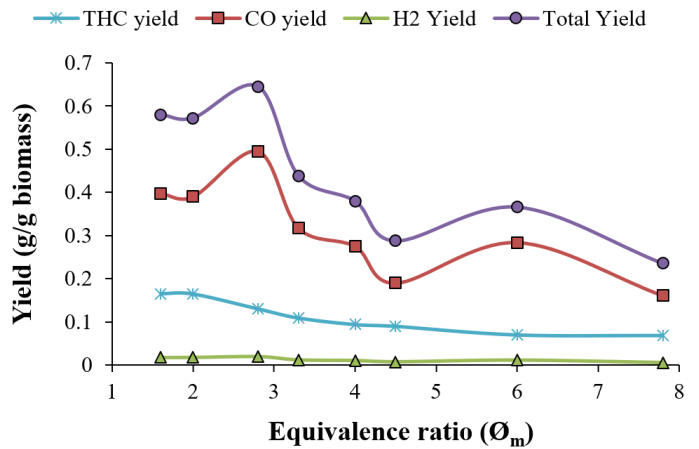Fig. 23 Total HRR by biomass mass loss rate and GHV in MJ/kg$_{biomass}$

Fig. 24 Yield of CO, THC, H$_2$ and their total v. $\varnothing_m$

All the emissions were averaged over the 300-500s test period. The rich fire equivalence ratio was varied by changing the air flow and $\varnothing_m$ as a function of the air flow is shown in Fig. 21. This is too wide a range of $\varnothing_m$ as it will be seen that the opimum is close to $\varnothing_m$ and an investigation range from 1.5 – 5 would be sufficient to determine the optimum for most biomass.

The primary and secondary HRR as a proportion of the total HRR is shown in Fig.22 as a function of $\varnothing_m$. The primary heat release generates the rich burn gasification temperature and this decreases as $\varnothing_m$ increases. However, as Fig. 19 shows the adiabatic flame temperature decreases as the mixture becomes richer. This results in an optimum $\varnothing_m$ for best release of gases and this is shown below to be 2.8 for pine wood, which is a primary HRR of 30 kW/m^2, as shown in Fig. 22.

The total HRR is shown in Fig. 23. The total HRR has two peaks and the first is close to the $\varnothing_m$ where the equilibrium CO and H$_2$ are at a maximum in Fig. 19. The second peak in total HRR in Fig. 23 is due to the secondary combustion after the discharge from the chimney.

The mass yields of CO, THC and H$_2$ are shown in Fig. 24 together with their total. This shows that the peak mass of flammable gases from the rich burn gasification primary combustion occurs at $\varnothing_m = 2.8$, but is nearly as high down to $\varnothing_m$ of 1.6. Fig. 24 shows that the cumulative mass of all the gases (Fig. 24 total plus the mass of H$_2$O and CO$_2$) is in good

agreement with the load cell mass loss. This shows that the FTIR measurements are reliable. In other work on different biomass better agreement with the two masses have been achieved.
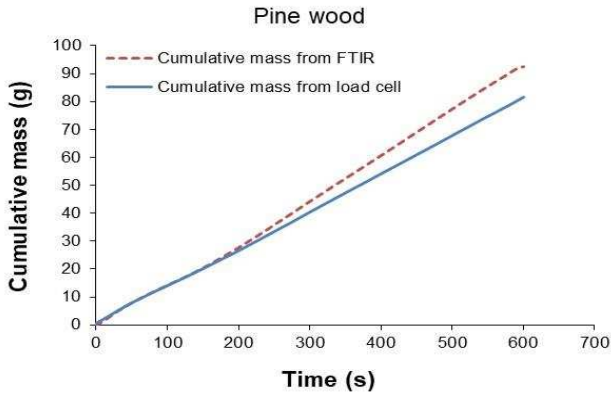
Fig. 25 Comparison of load cell measure biomass mass consumption and that derived from the mass emissions in Fig. 24.
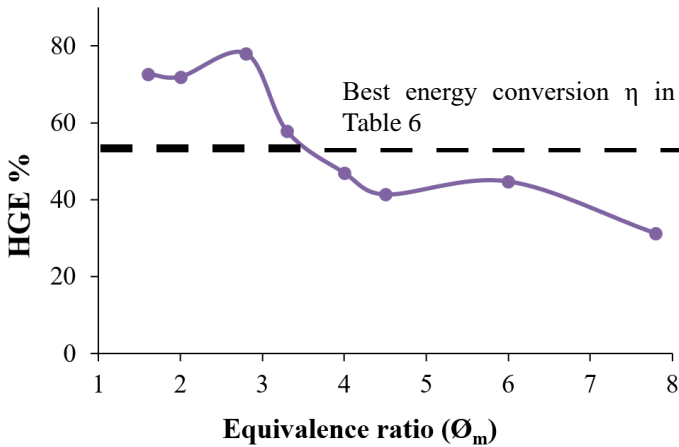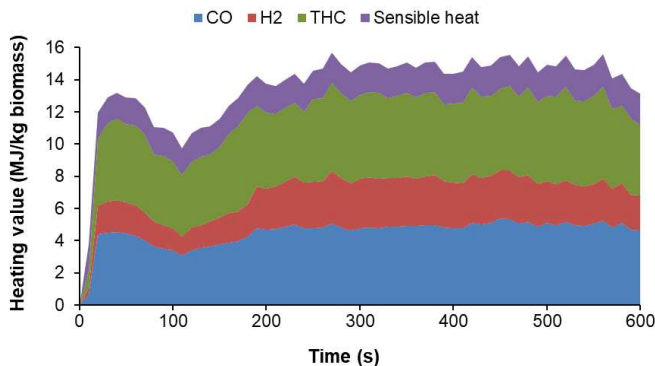

Fig.26. HGE as a function of $\emptyset_m$

Fig. 27 Heating value as function of time for air flow 19.2 g/(m².s), $\emptyset_m = 2.8$

The hot gas efficiency is a measure of the gasifier efficiency defined as:

$$HGE =$$

$$\frac{(HHV\ of\ the\ product\ gases + Sensible\ heat\ of\ the\ gases)(\frac{MJ}{kg\ biomass})}{HHV\ of\ the\ Fuel\ (\frac{MJ}{kg\ biomass})}$$

The HHV of the product gases is from Fig. 24 with the mass emissions multiplied by the HHV for each gas component and the total MJ are then divided by the mass in the original
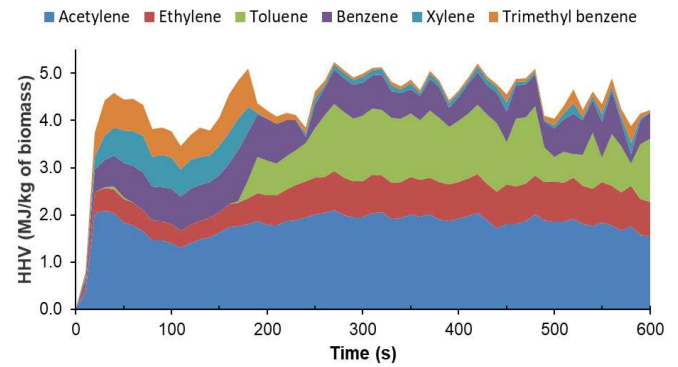

Fig. 28 Energy contribution in Fig. 27 for individual hydrocarbons.

biomass fuel. The HGE is shown as a function of $\emptyset_m$ in Fig. 26 where the peak is 78% at $\emptyset_m = 2.8$.

Fig. 27 shows the main contributors to the energy in the transfer chimney from the rich burn gasifier. As well as the energy of H_2, CO and THC there is the sensible heat which was calculated from the temperature of chimney gases and the total mass flow (air plus biomass mass consumption rate). The hydrocarbons are a major proportion of the efficiency and the main contributors to the hydrocarbon energy are shown in Fig. 28 and are acetylene, ethylene, toluene, benzene, xylene and trimethyl-benzene. The latter two components are the only ones in the gas composition from heating the biomass in nitrogen in Fig. 16 and these are minor components of the gasified gas energy. These hydrocarbon gases, particularly acetylene and ethylene have not been identified previously in gasifier gas composition and it is concluded that operation of the gasifiers at higher temperatures >800°C will thermally decompose these gases.

Fig. 26 compares the HGE with the maximum 54% energy conversion efficiency from heating the biomass at 25 kW/m² in nitrogen, as shown in Table 6. However, for $\emptyset_m$ in the range 1.6 – 2.8 the HGE is significantly higher and is contributed to by the extra CO and H_2 generated by the water and CO released below the char layer, where the cooler biomass gases interact with the char and undergoes the first two reactions in Table 4. Annex A shows that the HGE of 78% compares favorably with biomass gasifier thermal efficiencies in the literature. These range from Lepsy and Chmielnik [25] at 72% to 62% for Gordillo et al. [26] who optimised the gasification zone at $\emptyset_m = 3$, which is close to the present work. Not all the investigators in Annex A expressed their gasifier gas production as energy out in the gas to energy in the biomass, but sufficient information was included in the references for this to be calculated. The performance of the present type of rich log burning fixed bed gasifier with wet biomass is thus as good the best gasifiers in the literature, if they are controlled to be at the optimum $\emptyset_m$. Annex A also show that there are several poor performing biomass gasifiers in the literature.

To utilize this high 78% gasification efficiency the gases have to be transferred to the micro-gas turbine with no thermal losses and no condensation of the hydrocarbons. This is not a problem in furnace applications for heat, such as in Fig. 1 but needs careful engineering for engine applications of the

gasified biomass. To achieve this high gasification efficiency the rich burn $\emptyset_m$ has to be at the optimum of 2.8. To control this a thermal should be inerted in the gasifier output and the air flow to the gasifier controlled to achieve the condition where the gasifier temperature does not fall sharply as the air is increased, as shown in Fig.19. This optimum will be different for different biomass, due to the different elemental compositions.

Comparison of the gas composition for the optimum $\emptyset_m$ for pine in Annex A with other gasifiers shows CO content within the range from other biomass gasifiers, but there were some key differences. The hydrogen was lower and the water vapour was higher than most other biomass gasifier compositions in Annex A. This is because there was reduced high temperature water gas shift reaction as there was no steam injection to convert CO and H_2O into hydrogen. Also, there was high inert water content from the water in the biomass and from the reduced water gas shift reaction at the lower temperatures of this work. However, the greatest difference from other studies is the much higher hydrocarbons which contain a lot of the energy of the gas. This represents inefficient gasification as normally at higher temperatures these hydrocarbons would be burnt to produce CO and hydrogen.

CONCLUSIONS

A method of investigated the conversion of biomass into a gas was developed using small scale solid pine wood rich combustion with radiant energy heating. A modified cone calorimeter was used that enabled the gases evolved from the gasification zone to be measured using a heated calibrated Gasmet FTIR. The gas conversion was determined in nitrogen (devolatilisation) and air (rich burning). With a nitrogen at 25 kW/m^2 heating the volatiles had 54% of the energy of the pine biomass. With air at 70 kW/m^2 the thermal efficiency increased to 78% at $\emptyset_m$ of 2.8. Major gaseous components were H_2O, CO_2, CO with hydrocarbons acetylene, ethylene, benzene, toluene, trimetylbenzene and xylene. The conversion efficiency was reduced if leaner or richer $\emptyset_m$ was used and so control of the rich burning primary combustion air flow was critical. This optimum condition would be dependent on the biomass composition. The results showed that conversion of biomass into a gas with a high efficiency was feasible and this could be adapted to fuel a micro gas turbine for local power generation.

REFERENCES

[1] Trapp, C., de Servi, C., Casella, F., Bardow, A. and Colonna, P. (2015). Dynamic modelling and validation of pre-combustion CO_2 absorption based on a pilot plant at the Buggenum IGCC power station. International Journal of Greenhouse Gas Control 36, 13–26.

[2] Department-of-Energy-and-Climate-Change., Digest of United Kingdom Energy Statistics (DUKES), UK, 2017.

[3] Department-of-Energy-and-Climate-Change., Digest of United Kingdom Energy Statistics (DUKES), UK, 2015.

[4] Saeed, M.A., Irshad, A., Andrews, G.E., Phylaktou, H.N. & Gibbs, B.M. Agricultural waste biomass energy potential in Pakistan. Proceedings of the International Bioenergy (Shanghai) Exhibition and Asian Bioenergy Conference, European Biomass and Energy Conference (EUBCE), 2015. Shanghai, China,
DOI: http://dx.doi.org/10.5071/IBSCE2015-1CO.1.2

[5] Glas, L.A.S. (2017). Log wood boilers. 2017 http://www.glas.ie/wp-content/uploads/2011/01/GLAS Brochure-log-boilers.pdf.

[6] Schultz, M. Presentation on GE IGCC GTs on the Leeds CPD course on Ultra Low NOx GT Combustion, Jan, 2016.

[7] Irshad, A., Andrews, G.E., Phylaktou, H.N., B.M. Gibbs. (2019). Development of the controlled atmosphere cone calorimeter to simulate compartment fires. Proc. 9th International Seminar on Fire and Explosion Hazards, St. Petersburg, Russia.

[8] V. Babrauskas. (1993). Ten Years of Heat Release Research with the Cone Calorimeter. Proc. First Japan Symposium on Heat Release and Fire Hazards.

[9] B. Schartel, T.R. Hull, Development of fire-retarded materials—Interpretation of cone calorimeter data, Fire and Materials, 31 (2007) 327-354.

[10] M. Werrel, J.H. Deubel, S. Krüger, A. Hofmann, U. Krause, The calculation of the heat release rate by oxygen consumption in a controlled-atmosphere cone calorimeter, Fire and Materials, 38 (2014) 204-226.

[11] P.M. Lv, Z.H. Xiong, J. Chang, C.Z. Wu, Y. Chen, J.X. Zhu, An experimental study on biomass air–steam gasification in a fluidized bed, Bioresource Technology, 95 (2004) 95-101.

[12] M.A. Saeed, G.E. Andrews, H.N. Phylaktou, B.M. Gibbs, Global kinetics of the rate of volatile release from biomasses in comparison to coal. Fuel, 181 (2016) 347-357.

[13] A. Irshad, Andrews, G.E., Phylaktou, H.N., Gibbs, B.M. Development of the controlled atmosphere cone calorimeter to simulate compartment fires. in 9th International Seminar on Fire and Explosion Hazards. St. Petersburg, Russia.

[14] Daham, B.K., Andrews, G.E., Li, H., Ballesteros, R., Bell, M.C., Tate, J.E. and Ropkins, K. Application of a portable FTIR for measuring on-road emissions, 20 pp. SAE Paper 2005-01-0676. *In 'Emissions Measurement and Testing 2005' SAE SP*-1941, p.171-192, ISBN 0-7680-1586-3, (2005).

[15] H. Li, K. Ropkins, G.E. Andrews, B. Daham, M. Bell, J. Tate, G. Hawley. (2006). Evaluation of a FTIR Emission Measurement System for Legislated Emissions Using a SI Car. SAE Paper 2006-01-3368. Proceedings SAE

Powertrain Fluid Systems Conference, Toronto. ISBN 0-7680-1803-X, 2006.

[16] Alarifi, A., Phylaktou, H.N., Andrews, G.E. (2015). Toxic Gas Analysis from Compartment Fires using Heated Raw Gas Sampling with Heated FTIR 50 Species Gas Analysis. Proc. International Fire Safety Symposium. 2015. Coimbra, Portugal.

[17] Aljumaiah, O., Andrews, G.E., Abdullahi, A., Mustafa, B.G., Phylaktou, H.N. (2010). Wood Crib Fires under High Temperature Low Oxygen Conditions. Proc. Sixth International Seminar on Fire and Explosion Hazards. 2010. University of Leeds, UK.

[18] Gasmet Technologies Oy. (2010). Gasmet Calcmet for windows - User's guide and refernce manual. Helsinki, FINLAND.

[19] ISO 19702 (2015). Guidance for sampling and analysis of toxic gases and vapours in fire effluents using Fourier Transform Infrared (FTIR) spectroscopy. International Organization for Standardization: Geneva.

[20] Spindt, R.S., (1965) Air-fuel ratios from exhaust gas analysis. SAE Technical Paper SAE 650507.

[21[Chan, S.H. (1996). An Exhaust Emissions based Air-Fuel Ratio Calculation For Internal Combustion Engines. Proc. of the Institution of Mechanical Engineers, Part D: Journal of Automobile Engineering, **210**: p. 273-280.

[22] Zainal, Z.A., Ali, R., Lean, C.H., Seetharamu, K.N. (2001). Prediction of performance of a downdraft gasifier using equilibrium modeling for different biomass materials, Energy Conversion and Management, 42, 1499-1515.

[23] Babrauskas, V. (1984). Development of the cone calorimeter—A bench-scale heat release rate apparatus based on oxygen consumption, Fire and Materials, 8, 81-95.

[24] Gordillo, G., Annamalai, K., Carlin, N. (2009) Adiabatic fixed-bed gasification of coal, dairy biomass, and feedlot biomass using an air–steam mixture as an oxidizing agent. Renewable Energy Vol. 34, Issue 12, pp 2789-2797.

[25] Lepszy, S.and Chmielniak, T. (2010). Technical and economic analysis of biomass integrated gasification combined cycle. Proceedings of the ASME Turbo Expo Volume 1, 2010, Pages 631-637.

[26] Baldacci, A., Gradassi, A.T., Zeppi, C., Barducci, G.L., Daddi, P., Polzinetti, G. and Ulivieri, P. (1994). Syngas Production from Sorghum at Greve in Chianti Gasification Plant. Biomass for Energy Environment Agriculture and Industry. Proc. 8th European Biomass Conference Vol.3, Vienna, 3-5 Oct. 1994, p.1807-1813.

[27] Pinta, F. and Vergnet, L. Testing of Wood Gasification Pilot Plant for Industrial Heat Generation. Proc. 8th European Biomass Conference Vol.3, Vienna, 3-5 Oct. p.1791-1800.

[28] Porta, M., Traverso, A. and Marigo, L. (2006) Thermodynamic Analysis of a Small-Size Biomass Gasification Plant for Combined Heat and Distributed Power Generation. Proc. ASME Turbo Expo, Barcelona. ASME Paper GT2006-90918.

SURVEY OF SOME BIOMASS GASIFIER GAS COMPOSITIONS

GCV feed MJ/kg	Soft wood chips 19.6	Oak Dry 20.5	Sorghum Dry 14.3 17.4 daf	wood	wood	wood	Biomass 15.5	Dairy Biomass 21.5 daf	Pine Wood
Gasifier	Air	Air	Air	Air Fixed bed Updraft	Air Fixed bed downdraft	Air Fluidized Bed	Air Fixed bed updraft	Fixed Bed Updraft $\varnothing = 3$ Air/steam Steam/fuel 0.8	Air Fixed bed Updraft $\varnothing = 2.8$ No steam
CO%	16.0	18	14.6	24	21	14	27	11.5	14
H_2%	7.7 8.7dry	16	12.9 14.2 dry	11	17	9	17.3	25	8 10.4 (dry)
CO_2%	15.3	13	15.2	9	13	20	9.0	26	12
CH_4%	7.6	1.5	5.4	3	1	7	4.0	1.5	8% (THC)
H_2O%	11.0	-	9.4	-	-	-	4.1	-	23%
N_2%	41.5	48	42.3	53	48	50	38.6	36	35%
MW	-	24.8	25.4				24.05		~55
LHV MJ/m^3	5.59	4.8	5.35 6.52 dry	5.5	5.7	5.4		4.9	
LHV MJ/kg$_{gas}$	4.72	4.35	4.72 6.16 dry				5.38		
LHV MJ/kg$_{fuel}$	14.2	13.0	14.1 wet 18.5 dry				15.04		15.0
Efficiency %	72%	63.6 %	99% wet 106 dry				97%	62%	78%
Reference	Lepszy [25] 2010	Pinta [27] 1994	Baldacci [26] 1994	Gordillo [24] 2009	Gordillo [24] 2009	Gordillo [24] 2009	Porta [28] 2006	Gordillo [24] 2009	This work

Key: MW = Molecular Weight; LHV = Lower Heating Value; daf = dry ash free; THC total hydrocarbons (methane was zero)
Efficiency = kW gas energy output / kW biomass energy input